https://doi.org/10.1038/s40494-025-02203-x

Soil microbial and enzymatic signatures decode ancient millet fertilization strategies in Guanzhong arid farmlands

Zhizhen Feng[1,2], Xue Shang[3] ✉, Bo Li[1,2], Huiyong Ouyang[3,4], Yuxin Lu[1,2], Junchao Jia[1,2], Tao Qin[1,2], Hong Yan[1,2] & Jianqiang Liang[1,2]

Agricultural archaeology faces limitations in differentiating manure sources via stable isotopes (e.g., δ^{15}N). This study establishes a microbial-functional identification framework that deciphers prehistoric manuring strategies in Guanzhong dryland millet systems by linking microbial taxa to soil biochemistry. Pig manure (ZH) significantly enriched *Actinobacteria* (27.12%), elevating nitrate-N (10.54 mg·kg^{-1}) and Olsen P (151.13 mg·kg^{-1}), evidencing a "fast nutrient-*Actinobacteria* synergy" that archaeologically explains spatial co-occurrence of pig husbandry and millet storage. Sheep manure (YH) drove peak urease activity (1.64 mg·g^{-1}).) but depleted P (↓ 37.72% vs ZH), clarifying its rarity in archaeological records within calcareous soils. Cattle manure (NH) showed slow-release properties, aligning with modern topdressing. Chemical fertilizer (CF) reduced microbial richness by approximately 4.4% compared to organic manure treatments (based on ACE/Chao indices). Our manure identification framework re-orients agricultural archaeology from isotope tracing toward comprehensive integration of soil biochemical processes and microbial functional networks.

The transition from mobile foraging to sedentary agriculture in northern China during the late Neolithic period (ca. 5500-3000 BCE) was profoundly driven by the domestication and intensification of millet cultivation[1]. As the primary staple crop in the arid Loess Plateau, *Setaria italica* and *Panicum miliaceum* formed the ecological foundation for the rise of complex societies during the Bronze Age (ca. 2000-1500 BCE)[2]. Critically, integrated archaeobotanical and zooarchaeological evidence reveals that a transformative shift in millet agriculture from extensive cultivation to intensive cultivation coinciding with the emergence of swine husbandry[3]. This synergy is evidenced by the spatial co-occurrence of pig bone assemblages, granary structures, and archaeobotanic remains across multiple Neolithic sites[4,5], suggesting an integrated agro-pastoral system where livestock manure recycling directly supported crop productivity.

Stable nitrogen isotope (δ^{15}N) analysis has revealed elevated signatures in archaeological millet grains and human collagen, providing critical evidence for prehistoric manure application[6,7]. However, isotopic signatures are influenced by manure type (e.g., swine vs. cattle), application rates, mineralization pathways, and soil N-cycling dynamics[8–10]. δ^{15}N data alone cannot distinguish these variables. Also, this technology cannot resolve the underlying microbial consortia and enzymatic processes that drive nutrient transformations - the mechanisms essential for explaining the archaeologically observed swine-millet synergy.

To decode ancient fertilization strategies, integrating soil microbial ecology is imperative. Modern studies confirm that manure types exert distinct biogeochemical signatures through their influence on microbial consortia and enzymatic networks[11]. For instance, swine manure promotes nitrification via *Nitrosomonas*-dominated pathways, enhancing both δ^{15}N fractionation and plant-available nitrogen[12]. In contrast, cattle manure favors slower, fungal-mediated humification[13]. Moreover, manure specific microbiome shifts govern soil fertility outcomes. Swine manure selectively enriches *Actinobacteria* - keystone taxa for organic phosphorus mineralization and drought resilience, whereas cattle manure primarily favors *Proteobacteria* colonization[14,15]. These functional distinctions indicate that microbiome profiles may serve as bioindicators of ancient manure inputs, bridging archaeological patterns with agroecological mechanisms.

Although direct detection of past microbial communities remains challenging, modern analogues provide a powerful proxy framework that mechanistically links manure types and preservable soil functional signatures, such as extracellular enzyme activities and biogeochemical stoichiometry. This approach overcomes limitations inherent in isotopic

[1]Bio-Agriculture Institute of Shaanxi, Shaanxi, People's Republic of China. [2]Enzyme Engineering Research Center of Shaanxi, Shaanxi, People's Republic of China. [3]Department of Archaeology and Anthropology, University of Chinese Academy of Sciences, Beijing, People's Republic of China. [4]Key Laboratory of Vertebrate Evolution and Human Origins of Chinese Academy of Sciences, Institute of Vertebrate Palaeontology and Palaeoanthropology, Chinese Academy of Sciences, Beijing, People's Republic of China. ✉e-mail: shangxue@ucas.ac.cn

methods, particularly in contexts with depleted organic residues. It enables the inference of past land management practices through measurable biogeochemical mechanisms.

To address these interdisciplinary challenges, this study introduces a novel "SOIL PROCESS FINGERPRINTING" framework combining controlled field experiments with multi-proxy soil analyses. Simulating Neolithic practices in the Guanzhong dryland millet system, we assess swine (ZH), sheep (YH), and cattle (NH) manure impacts on urease and phosphatase kinetics (proxies for N/P mineralization), and 16S rRNA bacterial community composition. By correlating real-time enzymatic data with microbiome assemblies, we reconstruct the biogeochemical feedback that sustained ancient agroecosystems. This mechanistic approach complements and extends beyond first-year isotopic tracing (reported by Ouyang et al.[8]), offering new pathways to infer prehistoric resource management strategies.

Methods

Experimental site

The experiment was conducted at the Lintong Experimental Base of the Bio-Agriculture Institute of Shaanxi in Xi'an, Shaanxi Province (109°14'13.61"E, 34°29'51.49"N) over a continuous two-year cultivation cycle from June 2022 to September 2023. The area has a temperate continental monsoon climate, with an altitude of 360 m, annual precipitation of 591.8 mm, mean annual temperature of 13.5 °C, frost-free period of 219 days, and annual sunshine duration of 2052.7 h. The soil type is classified as brunisolic soil. Prior to the experiment, plow layer (0-20 cm) contained soil organic matter 16.51 $g{\cdot}kg^{-1}$, total nitrogen 0.74 $g{\cdot}kg^{-1}$, alkali-hydrolysable nitrogen 54.87 $mg{\cdot}kg^{-1}$, available phosphorus 24.26 $mg{\cdot}kg^{-1}$, available potassium 234.95 $mg{\cdot}kg^{-1}$, and pH 8.36. Throughout the two-year study, continuous millet monoculture was maintained with no other crops grown to preserve treatment integrity.

Experimental materials

Three types of animal manure (pig manure, sheep manure, and cattle manure) were selected and subjected to natural composting in the experimental area from during June 2022 to September 2023 until fully decomposed, without adding any composting agents or other substances, to simulate ancient manure fermentation. The specific nutrient contents of the three manures are shown in Table 1.

Given the prevalent use of chemical fertilizers in modern agriculture, a compound fertilizer (with an N-P_2O_5-K_2O ratio of 22-11-10) was chosen for the control treatment. The millet variety used (Jin Gu 21) was provided by the Millet Research Institute of Shanxi Agricultural University.

Experimental design

The experiment consisted of five treatments replicated across two consecutive growing seasons (2022–2023) with identical application protocols: three organic fertilizers (pig manure, sheep manure, and cattle manure), a compound fertilizer treatment, and a no-fertilizer control (see Fig. 1 for details). Each treatment was replicated three times, resulting in 15 experimental plots. Each plot measured 12.5 m^2, with a total experimental area of 187.5 m^2. Isolation zones were established between adjacent plots to prevent interaction.

Experimental methods

Pig, sheep, and cattle manure were each applied as organic fertilizers at the standard quantity of 15 $t{\cdot}ha^{-1}$, while the compound fertilizer was applied at 0.675 $t{\cdot}ha^{-1}$. Before millet sowing, soil tillage was carried out to prepare the seedbed. The fertilizer quantity for each plot was determined based on plot area (12.5 m^2) and the specified application quantity. After thorough incorporation into the soil by plowing, millet was manually sown. All plots were subjected to uniform irrigation and daily management, with types and amounts of fertilizers being the sole variable. All fertilizers were applied as a single basal dose, with no supplemental applications post-sowing.

Sample collection

At millet maturity in September 2023, a stratified sampling protocol was implemented across the experimental plots. This hierarchical design yielded 9 composite samples per treatment for physicochemical assays and 18 individual samples per treatment for microbial sequencing.

Specifically, for physicochemical analysis during millet harvest (September 23, 2023), three composite samples per replicate plot were collected from the plow layer (0–20 cm) using an S-pattern quintuple sampling method with approximately 1 m between each sampling point. Each composite soil sample was homogenized by quartering to ~1 kg and then split into two portions: one fresh fraction for immediate analysis of ammonium-nitrogen (NH_4^+-N), nitrate- nitrogen (NO_3^--N), moisture content (MC), enzyme activities, microbial biomass carbon (MBC) and nitrogen (MBN); and one air-dried fraction for pH, soil organic matter (SOM), total nitrogen (TN), available phosphorus (Olsen P), and available potassium (Olsen K) analysis after grinding and sieving (<2 mm).

For microbial community profiling, six discrete rhizosphere soil samples per replicate plot were aseptically collected with sterile centrifuge tubes. These samples underwent immediate flash-freezing in liquid nitrogen followed by permanent storage at −80 °C until DNA extraction.

Sample analysis

Soil physicochemical properties were analyzed according to Bao Shidan's methodology[16]. Soil pH was measured potentiometrically in a 1:2.5 (w/v) soil-water suspension using a calibrated pH meter (PHSJ-5, Shanghai Precision & Scientific Instrument Co., Ltd., China); SOM was quantified by the potassium dichromate ($K_2Cr_2O_7$) oxidation-capacity method under external heating (150 °C, 5 min); TN was determined using a semi-micro Kjeldahl analyzer (FOSS Kjeltec 8400) (digestion at 380°C for 1.5 h, followed by steam distillation and titration); NH_4^+-N and NO_3^--N were extracted with 2 M KCl (soil: solution = 1:5) and analyzed by continuous flow analyzer (CFA) (AA3, SEAL Analytical); Olsen P was extracted with 0.5 M $NaHCO_3$ (pH 8.5) and quantified via molybdenum blue colorimetry at 880 nm; Olsen K was extracted with 1 M NH_4OAc (pH 7.0) and measured by flame photometry (FP6410, Eppendorf); MBC and MBN were analyzed using the chloroform fumigation-extraction method, where fumigated soils were extracted with 0.5 M K_2SO_4, with MBC determined by dichromate oxidation and MBN by micro-Kjeldahl distillation.

Soil enzyme activities were assessed according to Guan Songyin's protocols[17] with critical enhancements from modern assay kits (Suzhou Comin Biotechnology Co., Ltd., China): urease activity was quantified via phenol-sodium hypochlorite colorimetry (kit no. SUE-2-Y) at 630 nm after 24 h incubation with urea substrate (37°C), expressed as mg NH_3-$N{\cdot}g^{-1}{\cdot}24\ h^{-1}$, validated against glycine standards; sucrase activity was measured using the 3,5-dinitrosalicylic acid (DNS) method (kit no. SSC-2-Y) with glucose calibration at 540 nm (24 h incubation at 37 °C), expressed as mg glucose$\cdot g^{-1}{\cdot}24\ h^{-1}$; catalase activity was titrated with 0.02 M

Table 1 | Nutrient composition of fertilizers

Fertilizer	pH	Organic Matter ($g{\cdot}kg^{-1}$)	Total N ($g{\cdot}kg^{-1}$)	Total P ($g{\cdot}kg^{-1}$)	Total K ($g{\cdot}kg^{-1}$)	NO_3^--N ($mg{\cdot}kg^{-1}$)	NH_4^+-N ($mg{\cdot}kg^{-1}$)
NH	9.31	22.5	1.14	0.737	1.37	829.15	8.20
YH	9.07	22.1	1.20	1.646	1.49	674.51	10.54
ZH	10.12	57.2	2.29	2.392	1.40	2.17	1348.06
CF	4.80	0.20	23.1	5.695	6.78	10020.00	13043.33

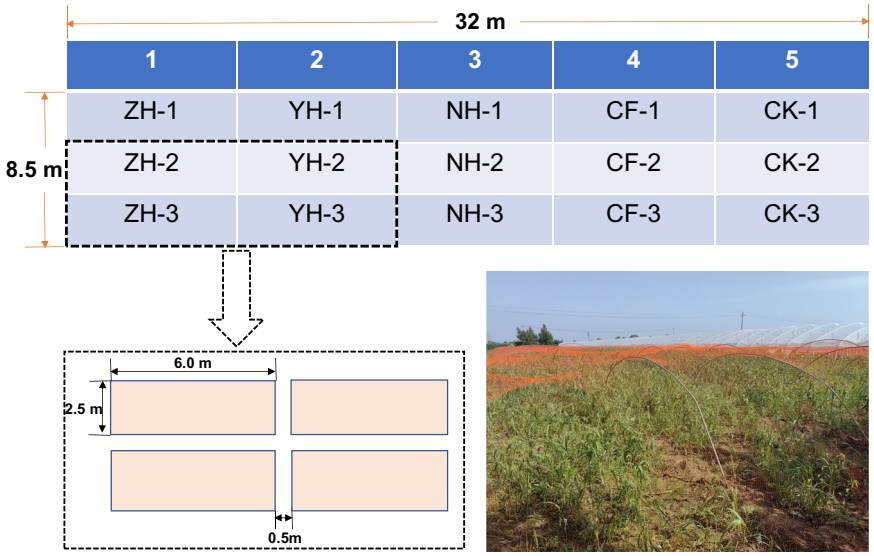

Fig. 1 | Layout schematic of the study area.

$KMnO_4$ after 20 min reaction with H_2O_2 (kit no. SCAT-2-Y), expressed as mL $KMnO_4 \cdot g^{-1} \cdot 20\ min^{-1}$; alkaline phosphatase activity utilized p-nitrophenyl phosphate hydrolysis (Kit no. SAKP-2-W).

Total genomic DNA was extracted from soil samples using the FastDNA™ SPIN Kit for Soil (MP Biomedicals, USA, Cat. No. 116560200) with optimized bead-beating parameters (2×45 s at 6.0 $m \cdot s^{-1}$). DNA concentration and purity were assessed via NanoDrop 2000 spectrophotometry (Thermo Fisher Scientific, USA, Waltham, MA). For microbial community profiling, the hypervariable V3–V4 regions of bacterial 16S rRNA genes were amplified using barcoded primers 338 F (5′-ACTCCTACGGGAGGCAGCAG-3′) / 806 R (5′-GGACTA CHVGGGTWTCTAAT-3′), followed by library preparation and paired-end sequencing (2×300 bp) on the Illumina MiSeq platform (Illumina Inc., USA). All library preparation and sequencing steps were performed by Majorbio Bio-Pharm Technology Co., Ltd. (Shanghai, China) under standardized protocols.

Statistical analysis

All experimental data were processed using SPSS 26.0 (IBM, USA). Considering the sample size of this study, differences among multiple groups were assessed using the non-parametric Kruskal–Wallis *H* test. Statistical significance was defined at $P < 0.05$. When the Kruskal–Wallis test indicated significant effects, post-hoc pairwise comparisons were performed using Dunn's test with Bonferroni adjustment.

For microbial community analyses, Alpha diversity indices (ACE, Chao1) were compared using ANOVA as described above. Redundancy analysis (RDA) was conducted to evaluate correlations between environmental variables and microbial communities, with significance of explanatory variables tested by Monte Carlo permutation.

Results

Effects of fertilization on soil physicochemical properties

As shown in Fig. 2, the Soil pH (8.29–8.55) and water content (38.10–39.70%) showed no significant differences ($P > 0.05$) among treatments, indicating that short-term manure application minimally altered basal soil properties. Significant variations were found in soil nutrient profiles. ZH demonstrated the most substantial improvement in readily available nutrients. Its NO_3^--N (10.54 $mg \cdot kg^{-1}$) and Olsen P (151.13 $mg \cdot kg^{-1}$) increased by 161.25% and 69.43% respectively, compared to CK. This notable surge in NO_3^--N is particularly remarkable given the inherently low nitrate levels in raw swine manure. This implies the existence of efficient mineralization pathways. YH led to an increase in SOM (21.63 $g \cdot kg^{-1}$) and TN (1.34 $g \cdot kg^{-1}$), but its Olsen P was significantly reduced to 94.13 $mg \cdot kg^{-1}$, which is 37.72% lower than that in ZH ($P < 0.05$). NH and CF had relatively weaker effects on stimulating readily available nutrients.

Response of microbial biomass carbon and nitrogen to fertilization

As shown in Fig. 3, MBC showed no significant differences among the treatments (289.82-389.63 $mg \cdot kg^{-1}$, $P > 0.05$), with the highest value observed in CK (389.63 $mg \cdot kg^{-1}$) and the best performance among manure treatments in ZH (370.43 $mg \cdot kg^{-1}$). MBN exhibited a significant gradient difference: CK (14.33 $mg \cdot kg^{-1}$) > ZH (11.47 $mg \cdot kg^{-1}$) ≈ YH (10.93 $mg \cdot kg^{-1}$) > NH (10.41 $mg \cdot kg^{-1}$) > CF (10.17 $mg \cdot kg^{-1}$). This indicates high C/N manure (NF) inhibited microbial nitrogen utilization. The MBC/MBN ratio of the ZH treatment (32.10) was significantly higher than that of the CK treatment (27.24) ($P < 0.05$), indicating that its microbial community relied more on carbon sources to maintain metabolic activity.

Divergent distribution patterns of soil enzyme activities

Manure types significantly regulated soil enzyme activities (Fig. 4). The YH treatment showed the highest activities of soil urease (1.64 $mg \cdot g^{-1}$), catalase (27.03 $mg \cdot g^{-1}$), and alkaline phosphatase (10.08 $mg \cdot g^{-1}$) among all treatments. Nevertheless, its Olsen P content (94.13 $mg \cdot kg^{-1}$) was significantly lower than that of the ZH treatment (151.13 $mg \cdot kg^{-1}$), indicating a decoupling of enzyme activities and phosphorus availability. The ZH treatment had the second-highest activity of soil sucrase activity (33.53 $mg \cdot g^{-1}$) after YH, while its alkaline phosphatase activity (8.91 $mg \cdot g^{-1}$) corresponded to the highest Olsen P content (151.13 $mg \cdot kg^{-1}$).

Effects of different manure applications on soil microbial community structure

Bacterial diversity analysis revealed that the ZH treatment yielded the highest species richness indices (ACE: 3064.41 ± 327.7; Chao1: 3044.68 ± 310.19), whereas CF significantly reduced microbial richness by 4.36–4.62% in ACE and Chao1 indices (Tukey HSD, $P < 0.05$). No significant differences were detected in diversity indices (Shannon/Simpson, $P > 0.05$).

At the phylum level (Fig. 5A), dominant taxa included *Actinobacteria* (21.84–27.12%), *Proteobacteria* (19.11–23.74%), *Acidobacteria* (10.99–21.98%), *Chloroflexi* (11.69–14.95%), and *Firmicutes* (5.17–10.74%). Fertilizer types induced divergent distribution patterns (in an order of high to low): *Actinobacteria* showed ZH > CK > CF > NH > YH; *Proteobacteria* showed ZH > YH > CF > NH > CK; *Acidobacteria* exhibited NH > CK > YH > CF > ZH; *Chloroflexi* followed NH > CF > CK > YH > ZH; *Firmicutes* displayed ZH > CK > YH > CF > NH.

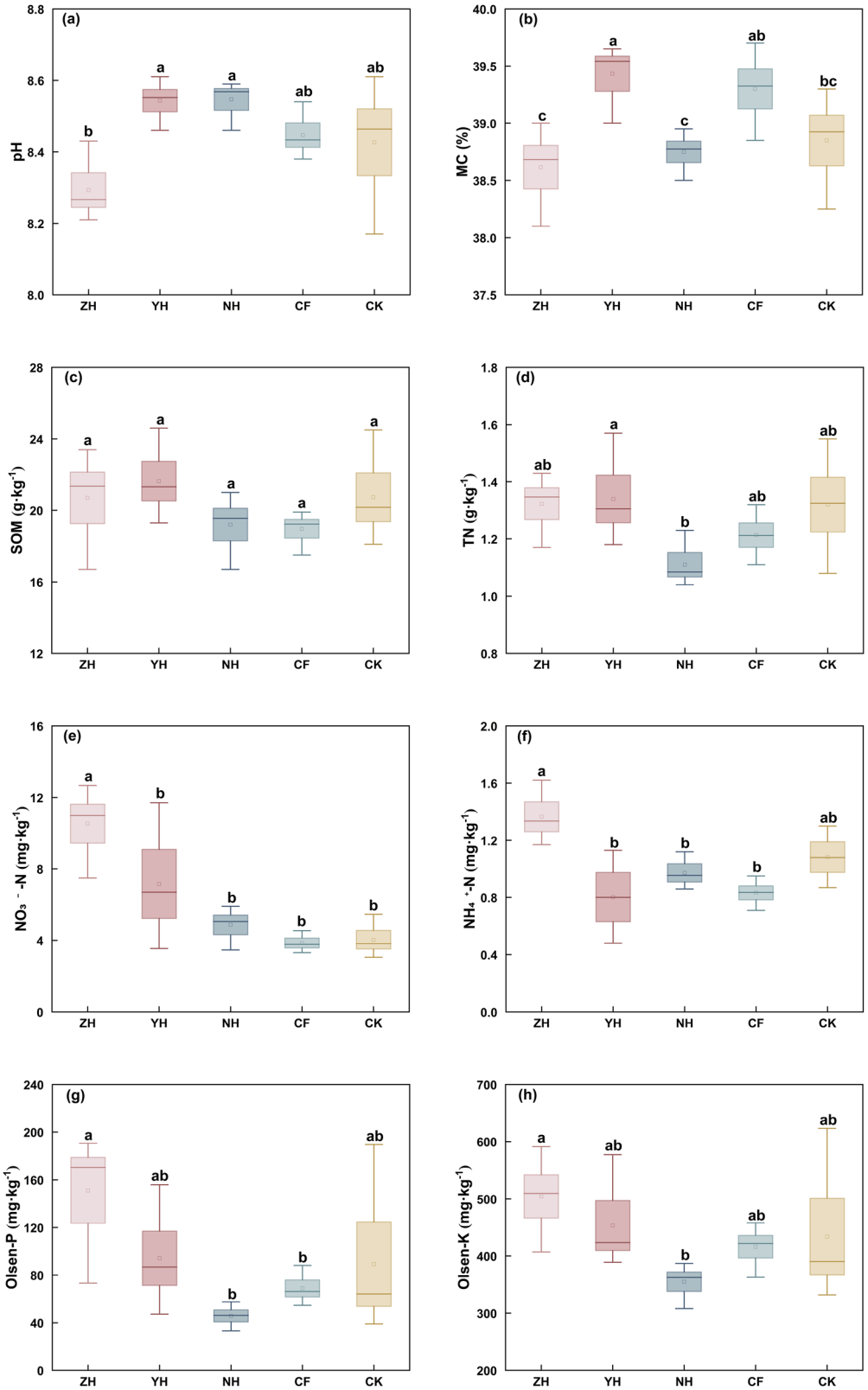

Fig. 2 | Manure-induced alterations in soil quality indices under fertilization regimes. a pH, (**b**) MC, (**c**) SOC, (**d**) TN, (**e**) NO_3^--N, (**f**) NH_4^+-N, (**g**) Olsen P, and (**h**) Olsen K. (MC = Moisture Content; SOC = soil organic matter; TN = total N, NO_3^--N = nitrate-N; NH_4^+-N = ammonium-N).

Critical functional shifts were observed. ZH treatment significantly enriched *Actinobacteria* (27.12%), *Proteobacteria* (23.74%), and *Firmicutes* (10.74%) while suppressing the relative abundance of *Acidobacteria* (10.99%) and *Chloroflexi* (11.69%), thereby shaping a microbial community structure optimized for nitrogen mineralization and phosphorus activation. YH treatment exhibited the lowest *Actinobacteria* abundance (21.84%) but elevated *Proteobacteria* (21.42%). NH treatment was characterized by dominance of *Acidobacteria* (21.98%) and *Chloroflexi* (14.95%).

At the genus level (Fig. 5B), the top 10 genera exhibited treatment-specific patterns that aligned with phylum-level shifts and soil nutrient

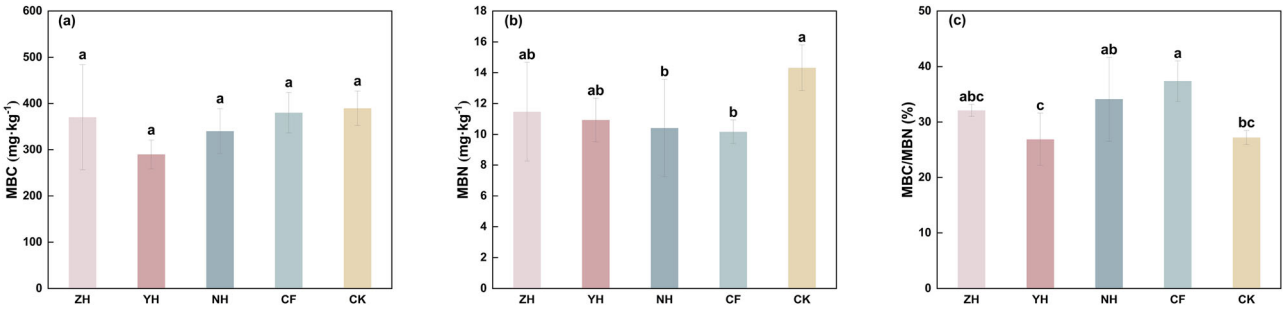

Fig. 3 | Manure-induced alterations in Microbial Biomass under fertilization regimes. a MBC, (**b**) MBN, and (**c**) MBC/MBN (MBC = Microbial Biomass Carbon; MBN = Microbial Biomass Nitrogen; MBC/MBN = MBC:MBN ratios).

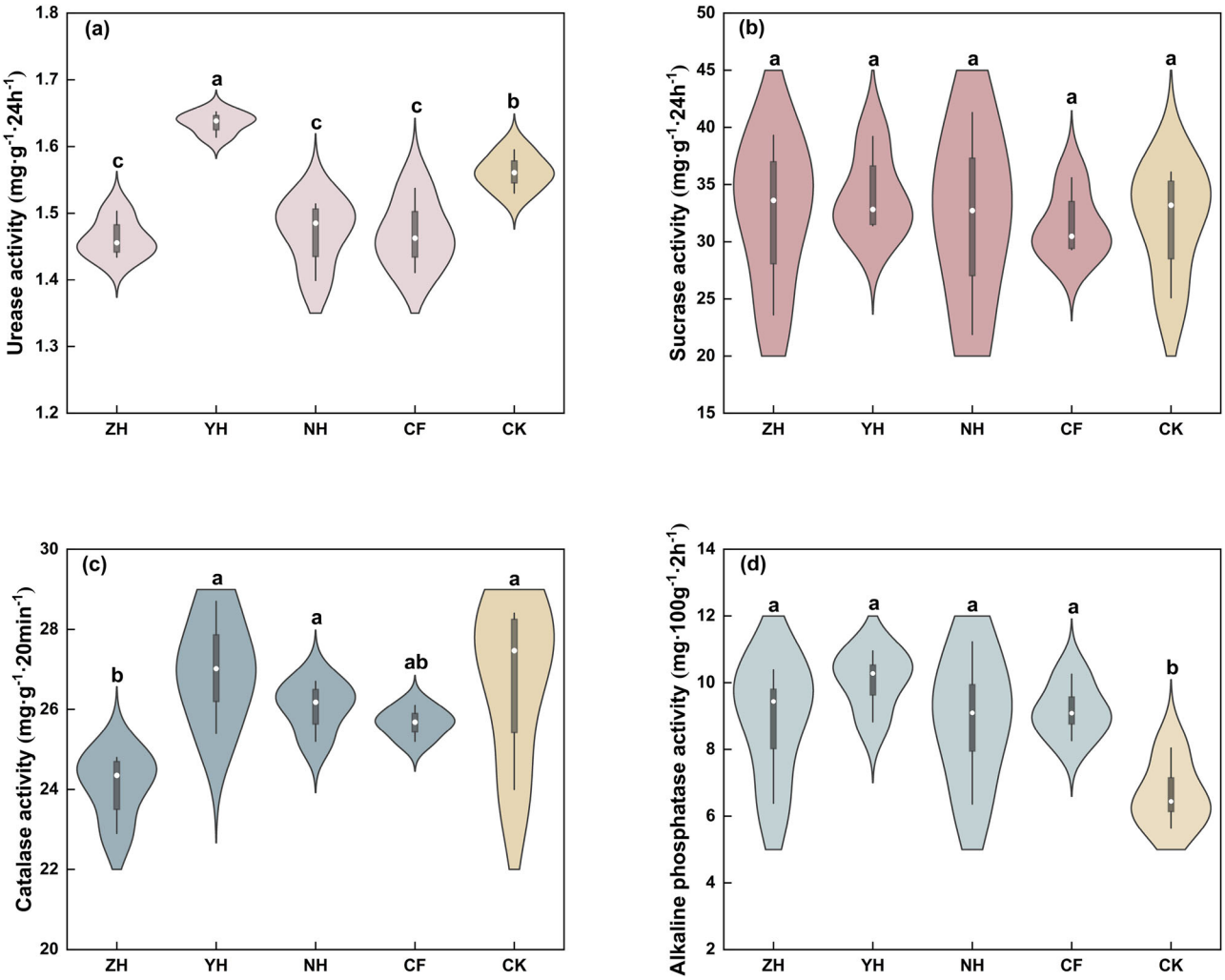

Fig. 4 | Dynamics of soil enzymatic profiles under different manure fertilization regimes. a urease activity, (**b**) sucrase activity, (**c**) catalase activity, and (**d**) alkaline phosphatase activity.

dynamics. The ZH treatment showed the highest relative abundance of *Bacillus* (5.14%) and *Sphingomonas* (2.80%), consistent with its superior phosphorus availability (Olsen P: 151.13 mg·kg^{-1}) and nitrogen mineralization (NO_3^--N: 10.54 mg·kg^{-1}). In contrast, *Vicinamibacterales* taxa were the most abundant in NH treatment (14.54%), corresponding to its *Acidobacteria*-dominated profile and oligotrophic characteristics. In the YH treatment, elevated *Geminicoccaceae* abundance (2.53%) co-occurred with the highest alkaline phosphatase activity (10.08 mg·g^{-1}) yet the lowest Olsen P content (94.13 mg·kg^{-1}), indicating that this taxon may drive microbial phosphorus immobilization rather than inorganic phosphorus release.

Interactive effects of environmental factors and microbial communities

Redundancy analysis (RDA) revealed that the first principal component (RDA1, 87.81%) and the second principal component (RDA2, 5.81%) collectively explained 93.62% of microbial community variation (Fig. 6), confirming environmental factors as dominant drivers of bacterial community assembly. Correlation analysis further demonstrated that Olsen P positively correlated with the relative abundances of *Proteobacteria* (Spearman r = 0.62, $P < 0.05$) and *Firmicutes* (r = 0.52, $P < 0.05$), while exhibiting a significant negative correlation with *Acidobacteria* (r = −0.53,

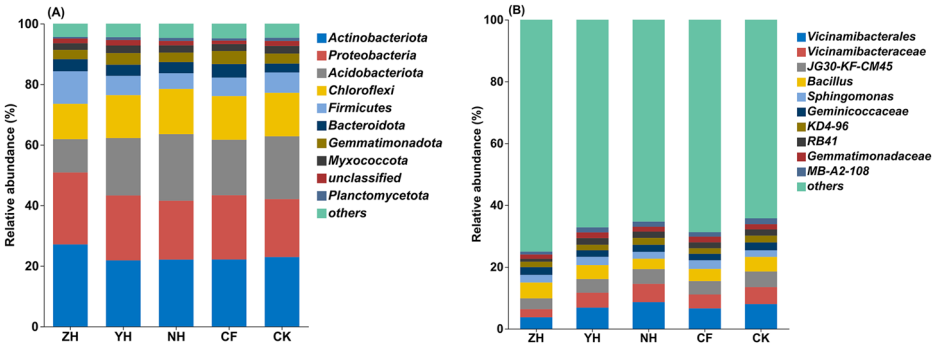

Fig. 5 | Soil bacterial community composition is altered by organic fertilization strategies. (**A**) phylum level and (**B**) genues leveltaxonomic profiles.

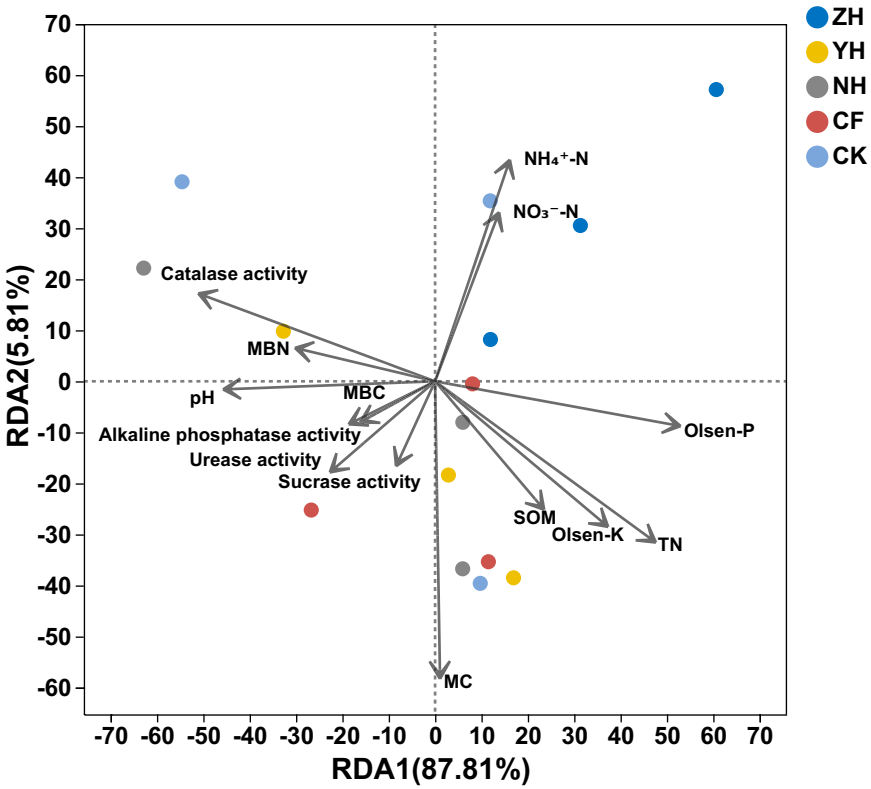

Fig. 6 | RDA ordination of bacterial phyla with environmental predictors.

$P < 0.05$). Catalase activity showed positive correlations with both *Acidobacteria* (r = 0.53, $P < 0.05$) and *Planctomycetota* (r = 0.61, $P < 0.05$) (Fig. 7).

The high-nutrient levels in the ZH treatment (e.g., Olsen P: 151.13 mg·kg^{-1}) were associated with the enrichment of *Proteobacteria* and *Firmicutes*, indicating that swine manure elevates soil nutrient availability to enhance proliferation of these phyla. Concurrently, ZH treatment significantly suppressed *Acidobacteria*, a response directly attributable to the established negative correlation between Olsen P and this phylum.

Discussion

In the calcareous soil (pH > 7.5) of the Guanzhong dryland region, manure type exerts significant differential regulation on soil functions. ZH enhances NO_3^--N (10.54 mg·kg^{-1}, ↑161.25% vs. control) and Olsen P (151.13 mg·kg^{-1}, ↑69.43% vs. control) through a synergistic mechanism: "quick nutrient release-*Actinobacteria* enrichment-enzymatic activation". This process is driven by *Actinobacteria*-secreted alkaline phosphatase (encoded by the *phoD* gene), which mineralizes organic phosphorus and dissolving mineral potassium via citrate metabolism, thereby establishing an available phosphorus reservoir[18,19]. At the genus level, this was specifically evidenced by the dominance of phosphate-solubilizing *Bacillus* (5.14%) and nitrogen-cycling *Sphingomonas* (2.80%), which directly contributed to enhanced phosphorus availability and nitrate accumulation[20,21]. The functional linkage between *Actinobacteria* abundance and Olsen P is further validated by redundancy analysis (RDA), which confirms a positive correlation between these parameters. This synergy provides diagnostic signatures for the microbial-functional identification framework. It explains the Neolithic spatial coupling of pig bones and millet storage pits observed across Yellow River floodplains[4,22]. Crucially, this mechanism precisely aligns with the nitrate preference of millet crops[10]. Another, δ^{15}N enrichment in Han Dynasty grains[23], provides direct isotopic evidence for intensified fertilization practices. Collectively, these findings confirm that ancient preferential selection of pig manure for soil function enhancement.

YH significantly enhanced urease (1.64 mg·g^{-1}) and phosphatase activities (10.08 mg·g^{-1}). However, its inherent oxalate residues[24] triggered oxalate-phosphate co-deposition in calcareous soils[25], suppressing colonization of the oxalate-degrading bacterium *Oxalobacter formigenes*. This resulted in oxalate accumulation, forming insoluble calcium oxalate precipitates, and ultimately reducing Olsen P (94.13 mg·kg^{-1}) by 37.72% compared to ZH treatment. Genus-level analysis revealed elevated

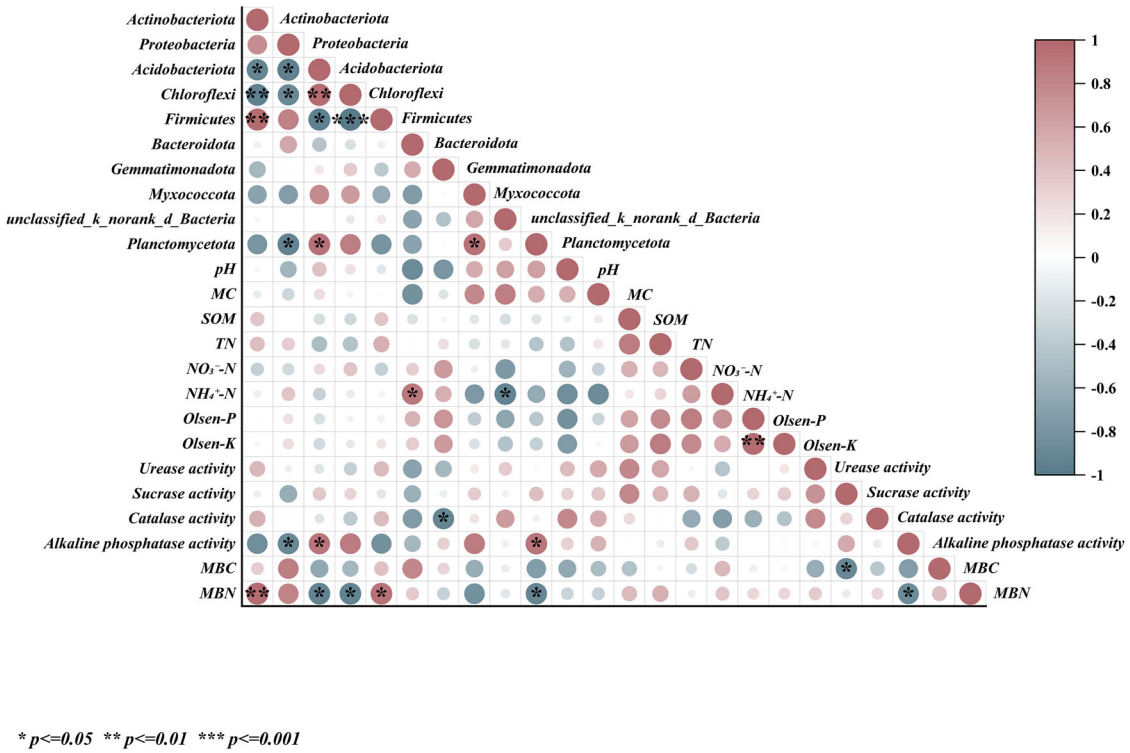

Fig. 7 | RDA heatmap of bacterial phylum-level abundance correlations with soil physicochemical properties and enzymatic activities under different fertilization treatments.

Geminicoccaceae-affiliated taxa (2.53%), which may facilitate organic matter decomposition without concomitant mineral phosphorus release[26], further exacerbating phosphorus limitation. This phosphorus immobilization explains the long-term functional degradation risk of sheep manure in phosphorus-deficient calcareous soils[27]. These findings suggest that ancient land-management strategies were not merely adaptations to husbandry constraints but were functionally guided by empirical observations of biogeochemical outcomes. The synergy between practical herding practices and nutrient immobilization phenomena offers an interdisciplinary framework for interpreting historical agricultural decision-making. It further aligns with the archaeological distribution of sheep manure deposits away from farming areas[28], reflecting ancient empirical knowledge of manure characteristics and zoned management.

NH characterized by high lignocellulose content and an elevated C/N ratio triggers microbial nitrogen competition[29,30], delaying nutrient release[31]. Its slow humification process relies on multi-stage fermentation driven by phyla like *Chloroflexi*, aligning with Han's "mid to late-stage fertilization" strategies that maintained stable $\delta^{13}C$ values despite aridification[23]. Genus level data confirm the dominance of oligotrophic taxa within *Vicinamibacterales* and *Vicinamibacteraceae*[32,33], which thrive under carbon-limited conditions and contribute to slow nutrient turnover. This mechanism enhances soil aggregate stability and stress resistance through slow-release nutrient provisioning[34,35]. These dynamics directly match historical records documenting cattle manure application during fallow periods[36], reflecting ancient adaptive management of slow-release fertilizers.

CF, due to its lack of organic matter, induced a loss of microbial diversity. This in turn reduced exopolysaccharide secretion and compromised soil aggregate stability[37,38]. In addition, soil acidification from chemical fertilizers inactivated alkaline phosphatase through conformational distortion and suppressed urease synthesis[39,40]. It also activated heavy metals (e.g., Cd^{2+}) that damaged microbial membrane integrity[41]. These interconnected processes established a vicious cycle of soil - ecosystem degradation. These findings together contrast sharply with organic manure systems that sustained soil functionality across dynastic transitions.

Microbial community structures critically amplified functional differentiation among manure types. ZH formed an *Actinobacteria-Proteobacteria-Firmicutes* consortium with high phosphatase activity and *Bacillus*-mediated drought resistance, synergistically elevating soil water retention and nutrient cycling[42]. This consortium drove the rapid-P-N synergy (Olsen P: 151.13 mg·kg^{-1}; NO_3^--N: 10.54 mg·kg^{-1}) but exhibited lower urease activity (1.64 mg·g^{-1}). than YH, confirming *Actinobacteria*'s specialization in phosphorus cycling over nitrogen transformation.

In YH, while *Actinobacteria* abundance was minimal (21.84%), it enriched highly functional *Proteobacteria* (21.42%). Specifically, *β-Proteobacteria* (e.g., *Rhodocyclaceae*) exhibited robust *ureC* gene expression[43], directly driving peak urease activity (1.64 mg/g). However, the proliferation of *Acidobacteria* (18.97%) and oxalate-induced phosphorus fixation[44] reduced Olsen P by 37.72% versus ZH, establishing a distinct tradeoff regime of "nitrogen-transformation/phosphorus -immobilization". The prominence of *Geminicoccaceae*-related genera further supports this functional trade-off, highlighting their role in organic matter decomposition without proportional phosphorus mineralization[26].

By contrast, cow manure driven oligotrophic communities (*Acidobacteria* and *Chloroflexi*)[45] suppressed urease synthesis via quinone metabolism[46] and upregulated lignin peroxidase (*lip*) genes to build recalcitrant carbon pools[47]. Genus-level patterns dominated by uncultured *Vicinamibacterales* and KD4-96 taxa reinforce the slow-decay characteristics of this regime, yielding a slow carbon release and low available nutrient regime, evidenced by lower ACE diversity (2890.91 vs. ZH's 3064.41).

Based on these mechanistic divergences, we propose an archaeological microbial-functional identification framework using signature combinations for manure tracing. This functional microbiome approach is complementary, not competitive to isotopic analyses. Its decisive merit lies in the persistence of microbial functional signals even in organically depleted contexts, where conventional isotopic methods face limitations due to the absence of well-preserved residues like charred grains or bones. This framework extends analytical capacity to previously inaccessible archaeological scenarios. Critically, this framework operates not through direct measurement of past microbiota, but by interpreting preservable functional

residues (e.g., enzyme-metal complexes, lipid biomarkers, and biogeochemical stoichiometry). These signatures are decoded using the mechanistic relationships established in this study. While the framework offers these advantages, its archaeological accuracy may be compromised by temporal soil discrepancies, such as microbial community succession[48], organic matter variability[49], and pH fluctuations[39,40]. Furthermore, certain soil properties (e.g., organic carbon accumulation and aggregate stability) exhibit slower dynamics that may require longer-term observation to fully quantify their response to different manure types. To ensure reliability, robust validation through multi-dimensional cross verification is essential. This includes integrating metagenomic profiling of settlement-layer microbiota, long-term field experiments, soil isotopic signatures (e.g., δ^{15}N) coupled with elemental tracing, and spatial correlation analyses of farming remains.

Data availability

All data supporting this study's findings are presented in the manuscript.

Received: 30 June 2025; Accepted: 18 November 2025;
Published online: 01 December 2025

References

1. Hongo, H., Kikuchi, H. & Nas, H. Beginning of pig management in Neolithic China: comparison of domestication processes between northern and southern regions. *Anim. Front.* **11**, 30–42 (2021).
2. Lu, H. et al. Earliest domestication of common millet (*Panicum miliaceum*) in East Asia extended to 10,000 years ago. *Proc. Natl. Acad. Sci. USA* **106**, 7367–7372 (2009).
3. Stevens, C. J., Zhuang, Y. & Fuller, D. Q. Millets, dogs, pigs and permanent settlement: productivity transitions in Neolithic northern China. *Evol. Hum. Sci.* **6**, e44 (2024).
4. Yang, J. et al. Sustainable intensification of millet-pig agriculture in Neolithic north China. *Nat. Sustain.* **5**, 780–786 (2022).
5. Shelach-Lavi, G. How Neolithic farming changed China. *Nat. Sustain.* **5**, 735–736 (2022).
6. Wang, X. et al. Multi-Isotope analysis reveals human millet-based diets and limited mobility in the central plains of China ca. 5000 years ago. *Int. J. Osteoarchaeol.* **35**, e3407 (2025).
7. Christensen, B. T. et al. Manure for millet: Grain δ^{15}N values as indicators of prehistoric cropping intensity of *Panicum miliaceum* and *Setaria italica*. *J. Archaeol. Sci.* **139**, 105554 (2022).
8. Ouyang, H. et al. Experimental archaeological study in China: implications for reconstruction of past manuring and dietary practices indicated by δ^{15}N values of *Setaria italica* and *Panicum miliaceum*. *Herit. Sci.* **12**, 55 (2024).
9. 15w?>Kim, S. R. et al. Analysis of microbial communities in solid and liquid pig manure during the fertilization process. *Sci. Rep.* **14**, 72 (2024).
10. Bogaard, A. et al. Crop manuring and intensive land management by Europe's first farmers. *Proc. Natl. Acad. Sci. USA* **110**, 12589–12594 (2013).
11. Xu, Z. et al. Enhancing nitrogen transformation and humification in cow manure composting through psychrophilic and thermophilic nitrifying bacterial consortium inoculation. *Bioresour. Technol.* **413**, 131507 (2024).
12. Tian, X. et al. Enhancing nitrogen conversion and microbial dynamics in swine manure composting process through inoculation with a microbial consortium. *J. Clean. Prod.* **423**, 138819 (2023).
13. Semenov, M. V. et al. Mineral and organic fertilizers distinctly affect fungal communities in the crop rhizosphere. *J. Fungi* **8**, 251 (2022).
14. Tharek, M. & Mat Amin, N. Bacterial community structure of fresh and composted cattle manure revealed through 16S rRNA gene amplicon sequencing. *Microbiol. Resour. Announc.* **14**, e0109224 (2025).
15. Yang, M. et al. Dynamic changes in and correlations between microbial communities and physicochemical properties during the composting of cattle manure with *Penicillium oxalicum*. *BMC Microbiol.* **24**, 301 (2024).
16. Bao, S. D. *Soil Agricultural Chemical Analysis* 3rd edn (China Agriculture Press, 2000).
17. Guan, S. Y., Zhang, D. & Zhang, Z. *Soil Enzyme and its Research Methods* (Chinese Agricultural Press, 1986).
18. Chen, X. et al. Soil alkaline phosphatase activity and bacterial *phoD* gene abundance and diversity under long-term nitrogen and manure inputs. *Geoderma* **349**, 36–44 (2019).
19. Zhang, X. et al. Responses of absolute and specific soil enzyme activities to long term additions of organic and mineral fertilizer. *Sci. Total Environ.* **536**, 59–67 (2015).
20. Pang, F. et al. Soil phosphorus transformation and plant uptake driven by phosphate-solubilizing microorganisms. *Front. Microbiol.* **15**, 1383813 (2024).
21. Li, K. et al. Soil metagenomics reveals the effect of nitrogen on soil microbial communities and nitrogen-cycle functional genes in the rhizosphere of Panax ginseng. *Front. Plant Sci.* **15**, 1392883 (2024).
22. Pei, X. et al. A research about subsistence based on the animal remains in late Neolithic Sha Ying River Plain: A case from the Tuchengwang site, Henan Province. *Quat. Sci.* **44**, 480–498 (2024).
23. Liao, J. et al. Millet stable isotopes reveal the advance of agricultural practices in the core political regions of early imperial China. *CATENA* **257**, 109148 (2025).
24. Rahman, M. M., Abdullah, R. B. & Wan Khadijah, W. E. A review of oxalate poisoning in domestic animals: tolerance and performance aspects. *J. Anim. Physiol. Anim. Nutr.* **97**, 605–806 (2013).
25. Waldrip, H. M., He, Z. & Griffin, T. S. Effects of organic dairy manure on soil phosphatase activity, available soil phosphorus, and growth of sorghum-sudangrass. *Soil Sci.* **177**, 629–637 (2012).
26. An, Y. et al. Distinct rhizosphere soil responses to nitrogen in relation to microbial biomass and community composition at initial flowering stages of alfalfa cultivars. *Front. Plant Sci.* **13**, 938865 (2022).
27. Sigua, G. C., Williams, M. J. & Coleman, S. W. Long-term effects of grazing and haying on soil nutrient dynamics in forage-based beef cattle operations. *J. Sustain. Agric.* **29**, 115–134 (2007).
28. Chodorowski, J. et al. The content of phosphorus in mountain meadow (polonina) soils as an indicator of past shepherding activity. *Ekológia* **31**, 54–64 (2012).
29. Fernandez Dominguez, D. *Characterize and Control the Organic Matter Fate During Anaerobic Digestion to Optimize the Agronomic Value of Digestates* (PhD Thesis, Université de Montpellier, 2023).
30. Menzel, T., Neubauer, P. & Junne, S. Role of microbial hydrolysis in anaerobic digestion. *Energies* **13**, 5555 (2020).
31. Zhang, Z. et al. Aerobic co-composting of mature compost with cattle manure: Organic matter conversion and microbial community characterization. *Bioresour. Technol.* **382**, 129187 (2023).
32. Huber, K. J. & Overmann, J. *Vicinamibacteraceae* fam. nov., the first described family within the subdivision 6 *Acidobacteria*. *Int. J. Syst. Evol. Microbiol.* **68**, 2331–2334 (2018).
33. Kang, P. et al. A comparison of microbial composition under three tree ecosystems using the stochastic process and network complexity approaches. *Front. Microbiol.* **13**, 1018077 (2022).
34. Jiang, B. et al. Effects of nitrogen reduction combined with liquid cattle manure on dry matter accumulation, nutrient absorption and translocation of maize in cold regions after anthesis. *J. Northeast Agric. Univ.* **52**, 29–38 (2021). In Chinese.
35. Das, S., Liptzin, D. & Maharjan, B. Long-term manure application improves soil health and stabilizes carbon in continuous maize production system. *Geoderma* **430**, 116338 (2023).
36. Xiong, D. & Hui, F. On changes of manure in pre-modern China. *Stud. Hist. Nat. Sci.* **40**, 149–160 (2021).
37. Cai, F. et al. Bioorganic fertilizer maintains a more stable soil microbiome than chemical fertilizer for monocropping. *Biol. Fertil. Soils* **53**, 861–872 (2017).

38. Li, J., Shangguan, Z. & Deng, L. Dynamics of soil microbial metabolic activity during grassland succession after farmland abandonment. *Geoderma* **363**, 114167 (2020).
39. Geisseler, D. & Scow, K. M. Long-term effects of mineral fertilizers on soil microorganisms—a review. *Soil Biol. Biochem.* **75**, 54–63 (2014).
40. Zhang, L. et al. Effects of long-term application of nitrogen fertilizer on soil acidification and biological properties in China: a meta-analysis. *Microorganisms* **12**, 1683 (2024).
41. Li, D. et al. A global meta-analysis reveals effects of heavy metals on soil microorganisms. *J. Hazard. Mater.* **491**, 138018 (2025).
42. Liu, X. et al. Effects of exogenous organic matter addition on agricultural soil microbial communities and relevant enzyme activities in southern China. *Sci. Rep.* **13**, 8045 (2023).
43. AbdElgawad, H. et al. Actinomycetes enrich soil rhizosphere and improve seed quality as well as productivity of legumes by boosting nitrogen availability and metabolism. *Biomolecules* **10**, 1675 (2020).
44. Wang, Y. et al. Changes in rhizosphere phosphorus fractions and phosphate-mineralizing microbial populations in acid soil as influenced by organic acid exudation. *Soil Tillage Res.* **225**, 105543 (2023).
45. Bledsoe, R. B., Goodwillie, C. & Peralta, A. L. Long term nutrient enrichment of an oligotroph dominated wetland increases bacterial diversity in bulk soils and plant rhizospheres. *mSphere* **5**, e00817–e00820 (2020).
46. Rayne, N. & Aula, L. Livestock manure and the impacts on soil health: a review. *Soil Syst.* **4**, 64 (2020).
47. Li, J. et al. Pathways of soil organic carbon accumulation are related to microbial life history strategies in fertilized agroecosystems. *Sci. Total Environ.* **927**, 172191 (2024).
48. Zhu, Y. et al. A buried Neolithic paddy soil reveals loss of microbial functional diversity after modern rice cultivation. *Sci. Bull.* **61**, 1052–1060 (2016).
49. Cao, S. et al. Changes of soil bacterial structure and soil enzyme activity in Chinese fir forest of different ages. *Acta Ecol. Sin.* **41**, 1846–1856 (2021).

Acknowledgements

We extend our sincere gratitude to the Millet Research Institute, Shanxi Agricultural University/Shanxi Academy of Agricultural Sciences for providing germplasm resources and technical support in seed acquisition and characterization. We thank the Science and Technology Program of Shaanxi Academy of Sciences (Grant Nos. 2022K-02 and 2020K-15), National Natural Science Foundation of China (Grant No. 42277441), National Social Science Fund of China (Grant No. 21BKG040), Science and Technology Department of Shaanxi Province (Grant No. 2023-CX-PT-12), and Science and Technology Program of Xianyang (Grant No. L2022-QCYZX-NY-006) for research support.

Author contributions

All authors contributed to this study. Z.Z.F.: resources, supervision, data analysis, and writing-original draft. X.S.: methodology, supervision, writing review, editing, and project administration. B.L.: resources, supervision, and validation. H.Y.O.Y.: Investigation and data collection. Y.X.L.: investigation and data collection. J.C.J.: investigation and data collection. T.Q.: investigation and validation. H.Y.: investigation and data collection. J.Q.L.: investigation and data collection.

Competing interests

The authors declare no competing interests.

Additional information

Correspondence and requests for materials should be addressed to Xue Shang.